ISSN 1070-3284, Russian Journal of Coordination Chemistry, 2013, Vol. 39, No. 9, pp. 667–679. © Pleiades Publishing, Ltd., 2013.
Original Russian Text © M.E. Burin, T.V. Balashova, D.L. Vorozhtsov, A.P. Pushkarev, M.A. Samsonov, G.K. Fukin, M.N. Bochkarev, 2013, published in Koordinatsionnaya Khimiya, 2013, Vol. 39, No. 9, pp. 554–566.

ate Complexes of Lanthanides with Aryloxide Ligands: Synthesis, Structures, and Luminescence Properties

M. E. Burin, T. V. Balashova*, D. L. Vorozhtsov, A. P. Pushkarev, M. A. Samsonov, G. K. Fukin, and M. N. Bochkarev

Razuvaev Institute of Organometallic Chemistry, Russian Academy of Sciences, ul. Tropinina 49, Nizhni Novgorod, 603600 Russia

**e-mail: petrovsk@iomc.ras.ru*

Received February 18, 2013

Abstract—(2-Benzox(thi)azol-2-yl)phenolate and -naphtholate ate complexes of Sc, Y, La, Sm, Tb, and Yb are synthesized. The structure of (benzoxazolyl)phenolate complexes of La, Sm, and Yb are determined by X-ray diffraction analysis. All synthesized compounds manifest ligand-centered photo- and electroluminescence in a range of 510–540 nm. In addition, the spectra of the samarium and terbium complexes exhibit narrow bands of *f*–*f* transitions characteristic of Sm^{3+} and Tb^{3+} ions.

DOI: 10.1134/S1070328413090029

INTRODUCTION

The area of luminescent materials is one of the main fields among potential areas of application of rare-earth metal compounds, which is due to a unique property of Ln^{3+} ions to generate the narrow-band emission of *f*–*f* transitions.[1] The radiation wavelength can change from the near-UV to near-IR ranges depending on the lanthanide nature. Scandium, yttrium, and lanthanum containing no *f* electrons and lutetium with the filled *f* shell give no metal-centered luminescence. However, their derivatives are of significant interest as model compounds and potent ligand-luminescing fluorophores. In addition to the use of luminescent complexes in the biomedical sphere for the diagnostics of diseases and visualization of internal organs and tissues in living systems [1–4], much attention is given to their use as luminescent layers in organic light-emitting diodes (OLEDs) [5–7]. Neutral metal complexes with chelate ligands providing the enhancement of the emission of the lanthanide center are used in both cases. The mechanism of electric energy transformation into the light energy in OLED devices, being planar structures in which nanosized layers of hole transporting, luminescent, and electron transporting materials are arranged between the electrodes, includes stages of the injection of electrons and holes from the cathode and anode, respectively, into the organic layers and their concurrent migration under the external electric field and recombination in the luminescent layer with the formation of a photon. However, light-emitting structures of other type appeared in the recent time: they are similar to OLED in construction but differ basically in scheme of functioning. These devices were named light-emitting electrochemical cells (LEC) [8–13]. In these structures, the emission layer is formed of ionic metal complexes of the $[Ru(Bipy)]^{2+}(PF_6^-)_2$ type (Bipy is 2,2'-bipyridyl) [10]. Under the electric field action, the complexes dissociate to give independent ions that diffuse: anions diffuse to the cathode, and cations diffuse to the anode. Double layers with a high internal potential are formed in the near-electrode spaces providing an ohmic contact. The migration in the material of not electrons (as in OLED) but ions predetermines a number of advantages of LEC: a low (2–3 V) switch voltage and the efficiency of the device independent of the emission layer thickness and electrode material. However, a drawback is a long response time that depends mainly on the nature of diffusing ions. The cationic complexes of Os^{2+} [13], Ru^{2+} [10], Ir^{2+} [11], and Cu^{1+} [12] in which $[BF_4]^-$, $[PF_6]^-$, $[CF_3SO_3]^-$ anions are used as counterions serve as luminescent materials in LEC. According to our data, no anionic complexes with a cation as a counterion were applied in light-emitting devices. Data on the luminescence properties of the ionic rare-earth metal complexes are also lacking, although the formation of ate complexes is characteristic of organolanthanides [14].

We have earlier found that the neutral scandium complexes of the ScL_3 type and the most part of lanthanides of the $(L)_2Ln(\mu\text{-}L)_2Ln(L)_2$ type with (2-benzoxazol-2-yl)phenolate (OON) and (2-benzthiazol-2-yl)phenolate (SON) ligands and their naphtholate analogs (NpOON, NpSON) have the photo- (**PL**) and electroluminescence (**EL**) properties [15–17]. The

[1] Hereinafter, symbol Ln designates Sc, Y, La, and lanthanides.

Table 1. Elemental analysis results for complexes **I**–**XIV**

Compound (empirical formula)	Content (found/calculated), %			
	C	H	N	S
$Sc(OON)_4Li$ (I) ($C_{52}H_{32}N_4O_8LiSc$)	70.06/69.96	3.65/3.61	6.25/6.28	
$Sc(NpOON)_4Li$ (II) ($C_{68}H_{40}N_4O_8LiSc$)	71.74/71.69	4.97/4.97	4.54/4.54	
$Y(NpOON)_4Li$ (III) ($C_{68}H_{40}N_4O_8LiY$)	71.12/71.84	4.14/3.55	4.64/4.93	
$Y(NpSON)_4Li(DME)_2$ (IV) ($C_{76}H_{60}N_4O_8S_4LiY$)	65.51/66.08	4.26/4.38		9.02/9.28
$Tb(OON)_4Li(DME)_2$ (V) ($C_{60}H_{52}N_4O_{12}LiTb$)	60.76/60.71	4.41/4.42	4.74/4.72	
$Tb(SON)_4Li(DME)_2$ (VI) ($C_{60}H_{52}N_4O_8S_4LiTb$)	57.56/57.60	4.16/4.19		10.27/10.25
$Tb(NpOON)_4Li(DME)_2$ (VII) ($C_{76}H_{60}N_4O_{12}LiTb$)	65.95/65.80	4.40/4.36	4.06/4.04	
$Yb(NpOON)_4Li(DME)_2$ (VIII) ($C_{76}H_{60}LiN_4O_{12}Yb$)	64.83/65.14	3.73/4.32	4.15/4.20	
$Yb(NpSON)_4Li(DME)_2$ (IX) ($C_{76}H_{60}N_4O_8S_4LiYb$)	62.65/62.28	4.30/4.13		8.12/8.75
$Y(OON)_6Li_3$ (X) ($C_{78}H_{48}N_6O_{12}Li_3Y$)	68.36/68.33	3.55/3.53	6.15/6.13	
$Yb(OON)_6Li_3$ (XI) ($C_{78}H_{48}N_6O_{12}Li_3Yb$)	64.36/64.38	3.35/3.32	5.75/5.78	
$La(OON)_4Na(DME)_2$ (XII) ($C_{60}H_{52}NaO_{12}N_4La$)	70.01/60.92	4.46/4.43	4.79/4.74	
$Sm(OON)_4Na(DME)_2$ (XIII) ($C_{60}H_{52}NaO_{12}N_4Sm$)	60.39/60.33	4.42/4.39	4.69/4.69	
$Sm_2(NpOON)_7Li$ (XIV) ($C_{119}H_{77}N_7O_{14}LiSm_2$)	66.86/66.90	3.65/3.63	4.55/4.59	

luminescence spectra of the Pr, Nd, Sm, Ho, Tb, Er, Tm, and Yb complexes contain metal-centered emission bands along with bands of the organic groups. It seemed interesting to synthesize the luminescence spectra of the anionic lanthanide complexes containing the same ligands and an alkaline metal atom as a counterion. It was assumed that such compounds, similarly to the cationic *d*-metal complexes, would manifest specific EL properties. In this work, we report the synthesis of the ate complexes of Sc, Y, La, Sm, Tb, and Yb with substituted phenoxide and naphthoxide ligands and their structures and luminescence properties.

EXPERIMENTAL

The syntheses were carried out under the conditions excluding contact with air oxygen and moisture using the standard Schlenk technique. Dimethoxyethane (DME) was dried with sodium benzophenone ketyl using a standard procedure and sampled in vacuo prior to use. Tetrahydrofuran (THF) for spectral studies was purified by the treatment with NdI_2 as described earlier [18]. Silyl amides $Li[N(SiMe_3)_2]_3$, $Ln[N(SiMe_3)_2]_3$, (2-benzoxazol-2-yl)phenol, and (2-benzthiazol-2-yl)phenol were purchased from commercial sources, and (2-benzoxazol-2-yl)naphthol and (2-benzthiazol-2-yl)naphthol were synthesized by a described procedure [19].

IR spectra were recorded on an FSM-1201 FT-IR spectrometer in a range of 4000–400 cm^{-1}. Samples were prepared as suspensions in Nujol. Absorption spectra were measured on a PerkinElmer 577 spectrometer, and a PerkinElmer LS-55 spectrometer was used for recording emission spectra in the range from 200 to 800 nm. C,H,N elemental analyses were performed on a Euro EA 3000 analyzer (Table 1).

Three-layer OLED devices of the composition ITO/TPD/complex/Bath/Yb (ITO is indium–tin oxide (anode), TPD is N,N'-*bis*(3-methylphenyl)-N,N'-diphenylbenzidine (hole-transport layer), Bath is 4,7-diphenyl-1,10-phenanthroline (hole-blocking layer), and Yb is the cathode) were prepared by sputtering in a vacuum chamber at 10^{-6} Torr [20]. The thickness of the deposited layers was controlled using a quartz resonator. The EL spectra in the visible range and the volt–ampere (luminous) characteristics were obtained on a noncapsulated samples using a

USB-2000 fluorimeter (Ocean Optics), a PPE 3323 power source (GW Instek), and a GDM 8246 digital multimeter (GW Instek). The spectra and efficiency in the IR range were determined on a NIR-512 spectrometer (Ocean Optics) calibrated by an LS-1 CAL lamp (Ocean Optics).

Synthesis of $Sc(OON)_4Li$ (I). A solution of 2-(2-hydroxyphenyl)benzoxazole (257 mg, 1.22 mmol) in DME (5 mL) was added to a solution of $Sc[N(SiMe_3)_2]_3$ (160 mg, 0.30 mmol) and $LiN(SiMe_3)_2$ (51 mg, 0.30 mmol) in DME (10 mL). The reaction mixture was stirred for 15 min at 40–50°C. A finely crystalline yellow substance precipitated from the solution as the reaction mixture slowly cooled down. The solution was separated by decantation, and the precipitate was two times washed with cold DME and dried in vacuo. The yield of complex **I** was 231 mg (85%).

IR, ν, cm^{-1}: 3062 w, 1617 s, 1598 s, 1548 s, 1527 s, 1438 s, 1380 w, 1342 m, 1324 m, 1299 m, 1287 m, 1252 s, 1191 w, 1158 m, 1135 m, 1105 m, 1055 m, 1037 m, 1006 w, 968 w, 941 w, 923 w, 895 m, 874 s, 864 s, 845 m, 807 s, 710 m, 669 m, 637 m, 612 s, 591 m, 558 m, 538 w, 509 w.

Compound **V** was obtained similarly from $Tb[N(SiMe_3)_2]_3$ (157 mg, 0.25 mmol), $LiN(SiMe_3)_2$ (41 mg, 0.25 mmol), and 2-(2-hydroxyphenyl)benzoxazole (207 mg, 0.98 mmol) in a DME solution (15 mL). The yield of complex $Tb(OON)_4Li(DME)_2$ was 247 mg (85%).

The IR spectrum was identical to that compound **I**.

Synthesis of $Sc(NpOON)_4Li$ (II). A solution of HNpOON (0.2 mg, 0.76 mmol) in DME (3 mL) was added to a solution of $Sc[N(SiMe_3)_2]_3$ (0.09 g, 0.17 mmol) and $Li[N(SiMe_3)_2]$ (0.03 g, 0.18 mmol) in DME (2 mL). A light yellow substance began to precipitate immediately after mixing of the reactants. For the completeness of the reaction occurrence, the mixture was stirred at 70°C for 4 h. The precipitate was separated from the solvent by centrifuging, washed with DME (2 × 5 mL), and dried in vacuo. The yield of the product as a finely crystalline powder was 0.19 g (99%).

IR, ν, cm^{-1}: 1626 m, 1591 m, 1522 s, 1492 w, 1340 s, 1305 w, 1278 m, 1244 m, 1178 m, 1145 m, 1049 m, 922 w, 867 m, 836 m, 755 m, 634 s, 535 s.

Compounds **III**, **VII**, and **VIII** were synthesized similarly.

Complex **III** was obtained from HNpOON (0.13 mg, 0.49 mmol), $Y[N(SiMe_3)_2]_3$ (0.065 g, 0.11 mmol), and $Li[N(SiMe_3)_2]$ (0.02 g, 0.12 mmol) in DME (5 mL). The yield of $Y(NpOON)_4Li$ was 0.12 g (91%).

Complex **VII** was synthesized from $Tb[N(SiMe_3)_2]_3$ (0.064 g, 0.10 mmol), $Li[N(SiMe_3)_2]_3$ (0.017 g, 0.10 mmol), and HNpOON (0.12 g, 0.46 mmol) in a DME solution (5 mL). The yield of $Tb(NpOON)_4Li(DME)_2$ was 0.12 g (90%).

Complex **VIII** was synthesized from $Yb[N(SiMe_3)_2]_3$ (0.094 g, 0.14 mmol), $Li[N(SiMe_3)_2]_3$ (0.025 g, 0.15 mmol), and HNpOON (0.15 g, 0.57 mmol) in a DME solution (5 mL). The yield of $Yb(NpOON)_4Li(DME)_2$ was 0.18 g (93%).

The IR spectra of complexes **III**, **VII**, and **VIII** were identical to the spectrum of compound **II**.

Synthesis of $Y(NpSON)_4Li(DME)_2$ (IV). A solution of HNpSON (0.17 g, 0.62 mmol) in DME (3 mL) was added to a solution of $Y[N(SiMe_3)_2]_3$ (0.084 g, 0.15 mmol) and $Li[N(SiMe_3)_2]$ (0.026 g, 0.16 mmol) in DME (2 mL). The reaction mixture was stirred at 70°C for 4 h. A light orange precipitate was separated from the solvent by centrifuging, washed with DME (2 × 5 mL), and dried in vacuo. The yield of the product as a microcrystalline powder was 0.10 g (67%).

IR, ν, cm^{-1}: 1626 m, 1586 m, 1491 s, 1332 m, 1288 w, 1268 m, 1186 m, 1143 w, 945 m, 920 w, 863 m, 809 w, 756 s, 726 w, 630 w, 574 m, 468 m.

Compound **IX** was synthesized similarly from $Yb[N(SiMe_3)_2]_3$, (0.089 g, 0.14 mmol), $Li[N(SiMe_3)_2]_3$ (0.022 g, 0.14 mmol), and HNpSON (0.16 g, 0.58 mmol) in a DME solution (5 mL). The yield of $Yb(NpSON)_4Li(DME)_2$ was 0.146 g (71%).

The IR spectrum of complex **IX** was identical to that of compound **VIII**.

Synthesis of $Y(OON)_6Li_3$ (X). A solution of 2-(2-hydroxyphenyl)benzoxazole (389 mg, 1.84 mmol) in DME (5 mL) was added to a solution of $Y[N(SiMe_3)_2]_3$ (175 mg, 0.31 mmol) and $LiN(SiMe_3)_2$ (154 mg, 0.92 mmol) in DME (10 mL). The reaction mixture was stirred for 15 min at 40–50°C. Crystals of compound **X** precipitated from the solution as the reaction mixture slowly cooled down. The crystals were washed with cold DME (2 × 5 mL) and dried in vacuo. The yield of complex **X** was 337 mg (80%).

IR, ν, cm^{-1}: 3062 w, 1618 s, 1599 s, 1562 m, 1544 s, 1434 s, 1377 w, 1329 m, 1310 m, 1289 w, 1262 m, 1245 s, 1194 w, 1158 m, 1130 w, 1106 w, 1078 w, 1046 m, 1032 m, 1003 w, 944 w, 896 w, 863 s, 805 s, 757 s, 740 s, 705 m, 669 w, 637 m, 590 m, 550 w, 512 w.

Compound **XI** was obtained similarly from $Yb[N(SiMe_3)_2]_3$ (73 mg, 0.11 mmol), $LiN(SiMe_3)_2$ (56 mg, 0.33 mmol), and 2-(2-hydroxyphenyl)benzoxazole (141 mg, 0.67 mmol) in DME (15 mL). The yield of $Yb(OON)_6Li_3$ was 110 mg (69%).

The IR spectrum of complex **XI** was identical to that of compound **X**.

Synthesis of $Tb(SON)_4Li(DME)_2$ (VI). 2-(2-Hydroxyphenyl)benzothiazole (337 mg, 1.48 mmol) dissolved in DME (5 mL) was poured to a solution of $Tb[N(SiMe_3)_2]_3$ (237 mg, 0.37 mmol) and $LiN(SiMe_3)_2$ (62 mg, 0.37 mmol) in DME (10 mL). The reaction mixture was stirred for 15 min at 40–50°C. A precipitate was formed as the solution slowly cooled down. The precipitate was washed with cold DME several times and then dried in vacuo. The yield of complex **VI** was 385 mg (83%).

IR, ν, cm^{-1}: 3059 sh, 1600 s, 1550 m, 1494 m, 1320 s, 1283 m, 1201 m, 1154 w, 1044 w, 967 m, 874 m, 828 m, 748 s, 710 w, 591 w, 561 w, 547 w.

Synthesis of $La(OON)_4Na(DME)_2$ (XII). 2-(2-Hydroxyphenyl)benzoxazole (221 mg, 1.05 mmol) dissolved in DME (5 mL) was poured to a solution of $La[N(SiMe_3)_2]_3$ (162 mg, 0.26 mmol) and $Na[N(SiMe_3)_2]$ (48 mg, 0.26 mmol) in DME (10 mL). The reaction mixture was stirred for 15 min at 40–50°C. Crystals precipitated as the solution was slowly cooled down. The crystals were washed with cold DME several times and then dried in vacuo. The yield of complex **XII** was 260 mg (84%).

IR, ν, cm^{-1}: 3050 sh, 1611 s, 1601 m, 1557 m, 1538 s, 1476 s, 1352 m, 1337 m, 1319 w, 1287 w, 1245 s, 1190 w, 1156 m, 1134 w, 1075 w, 1046 m, 1033 w, 939 w, 894 w, 862 m, 805 m, 709 w, 631 w, 585 w, 550 w.

Compound **XIII** was synthesized similarly from $Sm[N(SiMe_3)_2]_3$ (137 mg, 0.21 mmol), $Na[N(SiMe_3)_2]$ (40 mg, 0.22 mmol), and 2-(2-hydroxyphenyl)benzoxazole (183 mg, 0.87 mmol) in DME (15 mL). The yield of complex **XIII** was 225 mg (87%).

The IR spectrum of compound **XIII** was identical to that of complex **XII**.

Synthesis of $Sm_2(NpOON)_7Li$ (XIV). A solution of $Sm[N(SiMe_3)_2]_3$ (107 mg, 0.17 mmol) and $LiN(SiMe_3)_2$ (28 mg, 0.17 mmol) in DME (10 mL) was added to a solution of 3-(2-benzoxazol-2-yl)-2-naphtholate (177 mg, 0.68 mmol) in DME (5 mL). The reaction mixture was stirred for 15 min at 40–50°C. Yellow crystals precipitated from the bright yellow solution as the reaction mixture slowly cooled down. The solution was separated by decantation, and the crystals were washed with cold DME several times and dried in vacuo. The yield of complex **XIV** was 143 mg (79%). Along with the crystals of compound **XIV**, LiNpOON was isolated in a quantitative yield (21 mg).

IR, ν, cm^{-1}: 3047 w, 1627 s, 1607 s, 1591 s, 1528 s, 1379 w, 1347 s, 1332 s, 1304 m, 1278 m, 1245 m, 1216 m, 1178 s, 1147 m, 1128 w, 1105 w, 1034 m, 1014 w, 918 w, 897 w, 862 m, 834 s, 782 w, 763 m, 692 w, 627 m, 548 w, 526 w, 502 m, 475 m.

X-ray diffraction analyses were carried out on Bruker AXS SMART APEX (for complexes **XII–XIV**) and Oxford Xcalibur Eos (for **X** and **XI**) automated diffractometers (graphite monochromator, MoK_α radiation, ω scan mode, λ = 0.71073 Å). Experimental sets of intensities were integrated using the SAINT [21] (for complexes **XII–XIV**) and CrysAlisPro [22] (for complexes **X** and **XI**) programs. The SADABS [23] (complexes **XII–XIV**) and SCALE3 ABSPACK [24] (complexes **X** and **XI**) programs were used for applying absorption corrections. The structures were solved by direct methods (SHELXTL) [25] and refined by full-matrix least squares for F^2_{nkl} in the anisotropic approximation for all non-hydrogen atoms. Hydrogen atoms were placed in the geometrically calculated positions and refined in the riding model. The main crystallographic characteristics and X-ray experimental parameters for compounds **X, XI**, and **XII–XIV** are listed in Table 2. Selected bond lengths and bond angles are given in Table 3. The structures were deposited with the Cambridge Crystallographic Data Centre (nos. 922899 (**X**), 922900 (**XI**), 922901 (**XII**), 922902 (**XIII**), and 922903 (**XIV**); deposit@ccdc.cam.ac.uk or http://www.ccdc.cam.ac.uk/data_request/cif).

RESULTS AND DISCUSSION

As we stated previously, the reactions of silyl amides $Ln[N(SiMe_3)_2]_3$ with phenols H(OON) and H(SON) or naphthols H(NpOON) and H(SON) in a ratio of 1 : 3 afforded monomeric $Sc(L)_3$ [26] or dimeric complexes $(L)_2Ln(\mu\text{-}L)_2Ln(L)_2$ [15–17] containing no coordinatively bound solvent, which often decreased the luminescence properties of the substances. The same method was used to synthesize the complexes containing lithium cations. In this case, four equivalents of phenol (naphthol) were added to lanthanide amide, and the reaction was carried out in the presence of one equivalent of lithium amide.

$$Ln[N(SiMe_3)_2]_3 + LiN(SiMe_3)_2 + 4HOAr \xrightarrow[-4HN(SiMe_3)_2]{DME} Ln(OAr)_4Li(DME)_x$$

(I–IX)

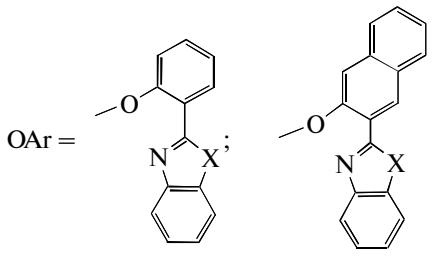

X = O (OON) **X** = O (NpOON)
X = S (SON) **X** = S (NpSON)

I: Ln = Sc, OAr = OON, $x = 0$
II: Ln = Sc, OAr = NpOON, $x = 0$
III: Ln = Y, OAr = NpOON, $x = 2$
IV: Ln = Y, OAr = NpSON, $x = 2$
V: Ln = Tb, OAr = OON, $x = 2$
VI: Ln = Tb, OAr = SON, $x = 2$
VII: Ln = Tb, OAr = NpOON, $x = 2$
VIII: Ln = Yb, OAr = NpOON, $x = 2$
IX: Ln = Yb, OAr = NpSON, $x = 2$

Table 2. Crystallographic data and the X-ray diffraction experimental and refinement parameters for complexes **X**–**XIV**

Parameter	Value				
	X	**XI**	**XII**	**XIII**	**XIV**
Formula weight	1551.19	1635.32	1182.96	1194.40	2309.70
Crystal system	Triclinic	Triclinic	Monoclinic	Monoclinic	Monoclinic
Space group	$P\bar{1}$	$P\bar{1}$	$P2/n$	$P2/n$	$P2_1/n$
a, Å	16.0382(4)	16.0814(2)	14.6695(8)	14.623(1)	15.6110(9)
b, Å	16.9905(8)	16.8680(3)	11.5330(6)	11.417(1)	24.941(1)
c, Å	17.6579(8)	17.6447(2)	15.4292(8)	15.386(2)	26.358(2)
α, deg	62.810(5)	62.871(1)	90	90	90
β, deg	64.035(3)	63.770(1)	90.105(1)	90.965(2)	101.568(1)
γ, deg	90.162(3)	89.896(1)	90	90	90
V, Å^3	3722.1(3)	3699.59(9)	2610.4(2)	2568.3(5)	10054.0(10)
Z	2	2	2	2	4
ρ_{calcd}, g/m^3	1.384	1.468	1.505	1.544	1.526
μ_{Mo}, mm^{-1}	0.858	1.339	0.897	1.223	1.235
F(000)	1604	1666	1208	1218	4688
Crystal size, mm^{-1}	0.40 × 0.15 × 0.15	0.40 × 0.20 × 0.20	0.28 × 0.25 × 0.13	0.25 × 0.21 × 0.15	0.30 × 0.30 × 0.08
θ Range, deg	3.41–26.00	2.92–26.00	1.92–26.00	1.91–26.00	1.68–26.00
Number of collected reflections	57628	23320	21832	14776	85665
Number of independent reflections (R_{int})	14586 (0.0871)	13635 (0.0761)	5111 (0.0310)	5012 (0.0625)	19741 (0.0444)
R_1/wR_2 ($I > 2\sigma(I)$)	0.0537/0.1203	0.0487/0.0740	0.0296/0.0742	0.0709/0.1811	0.0478/0.1037
R (for all data)	0.0804/0.1319	0.0774/0.0805	0.0350/0.0764	0.0880/0.1909	0.0598/0.1082
Goodness-of-fit	1.004	0.975	1.099	1.020	1.163
Residual electron density, e Å^{-3}	0.668/–0.836	1.995/–2.382	1.408/–0.741	4.290/–2.943	1.899/–1.668

The reactions readily occur in a DME solution at ambient temperature and give the expected products in a yield of 80–93%. Interestingly, the reaction of yttrium and ytterbium amides with H(OON) at the same ratio of the reactants affords complexes containing three lithium ions, $Y(OON)_6Li_3$ (**X**) and $Yb(OON)_6Li_3$ (**XI**), along with lithium-free neutral compounds $Yb_2(OON)_6$ and $Y_2(OON)_6$, whose yield is 56 and 49%, respectively. The reactions of Y or Yb amides with lithium amide and phenol in a ratio of 1 : 3 : 6 give compounds **X** and **XI** only in a yield of 70–80%. In the reactions involving amides of other lanthanides, the change in the ratio of the starting reactants does not change the composition of the products. In the most part of cases, the complexes evolved from the solution contain two molecules of the coordinatively bound solvent. The replacement of lithium amide in the initial mixture by sodium amide results in the sodium ate complexes $La(OON)_4Na(DME)_2$ (**XII**) and $Sm(OON)_4Na(DME)_2$ (**XIII**). The crystals of the complex of the fourth type, $Sm_2(NpOON)_7Li$ (**XIV**), were isolated in a yield of 79% along with Li(NpOON) from the reaction of samarium and lithium amides with naphthol H(NpOON) in a ratio of 1 : 1 : 4 at ambient temperature. All compounds were isolated as stable in air light yellow finely crystalline powders moderately soluble in THF and DME. It should be mentioned that, similarly to the neutral compounds containing no alkaline metal cation, the obtained products are sublimed in a high vacuum without decomposition; however, the coordinatively bound solvent is removed. The fact that the products of different compositions can be formed at the same ratio of the starting substances and under the same reaction conditions indicates, most likely, the influence of the Ln ion sizes on the formation of the complexes and some difference in the reactivity of the Ln–N bond for various lanthanides. It can be assumed that, at the initial stage in all reactions, amide is displaced by phenol (naphthol) to form lithium (sodium) phenoxide in which the N atom coordinatively interacts with the coordinatively unsaturated Ln atom in the starting amide $Ln[N(SiMe_3)_2]_3$ or in the formed intermediate $Ln[N(SiMe_3)_2]_2(XON)$. The formed N···Ln

Table 3. Selected bond lengths (Å) and bond angles (deg) in complexes **X**–**XIV**

X				**XI**			
Bond, Å		Angle, deg		Bond, Å		Angle, deg	
Y(1)–O(3)	2.240(2)	O(3)Y(1)O(11)	174.24(5)	Yb(1)–O(3)	2.212(2)	O(3)Yb(1)O(11)	174.46(6)
Y(1)–O(7)	2.243(1)	O(7)Y(1)O(11)	79.26(5)	Yb(1)–O(7)	2.214(2)	O(7)Yb(1)O(11)	79.05(6)
Y(1)–O(9)	2.253(1)	O(9)Y(1)O(11)	82.83(5)	Yb(1)–O(9)	2.219(1)	O(9)Yb(1)O(11)	83.51(6)
Y(1)–O(11)	2.250(2)	O(9)Y(1)O(5)	175.37(5)	Yb(1)–O(11)	2.219(2)	O(9)Yb(1)O(5)	175.80(6)
Y(1)–O(5)	2.254(1)	O(11)Y(1)O(5)	100.05(5)	Yb(1)–O(5)	2.230(1)	O(11)Yb(1)O(5)	98.76(6)
Y(1)–O(1)	2.260(1)	O(7)Y(1)O(1)	176.17(5)	Yb(1)–O(1)	2.234(2)	O(7)Yb(1)O(1)	175.80(6)
Li(1)–O(5)	1.940(4)	O(11)Y(1)O(1)	101.39(5)	Li(1)–O(5)	1.942(6)	O(11)Yb(1)O(1)	101.66(6)
Li(1)–O(3)	1.931(4)	O(9)Y(1)O(1)	78.45(5)	Li(1)–O(3)	1.955(4)	O(9)Yb(1)O(1)	78.79(5)
Li(1)–N(3)	2.007(4)	O(3)Y(1)O(5)	78.28(5)	Li(1)–N(3)	1.999(5)	O(3)Yb(1)O(5)	79.27(6)
Li(1)–N(2)	2.034(4)	O(5)Li(1)O(3)	94.3(2)	Li(1)–N(2)	2.004(5)	O(5)Li(1)O(3)	93.3(2)
Li(2)–O(11)	1.938(4)	O(5)Li(1)N(3)	91.8(2)	Li(2)–O(11)	1.882(4)	O(5)Li(1)N(3)	91.7(2)
Li(2)–O(7)	1.963(4)	O(3)Li(1)N(2)	91.0(2)	Li(2)–O(7)	1.955(5)	O(3)Li(1)N(2)	91.1(2)
Li(2)–N(6)	1.982(4)	O(11)Li(2)O(7)	94.6(2)	Li(2)–N(6)	1.990(4)	O(11)Li(2)O(7)	94.7(2)
Li(2)–N(4)	1.996(4)	O(7)Li(2)N(4)	90.5(2)	Li(2)–N(4)	2.019(4)	O(7)Li(2)N(4)	90.2(2)
Li(3)–O(1)	1.935(3)	O(11)Li(2)N(6)	93.0(2)	Li(3)–O(1)	1.909(4)	O(11)Li(2)N(6)	93.9(2)
Li(3)–O(9)	1.940(4)	O(1)Li(3)O(9)	94.9(2)	Li(3)–O(9)	1.926(4)	O(1)Li(3)O(9)	94.9(2)
Li(3)–N(1)	1.975(5)	O(9)Li(3)N(5)	92.4(2)	Li(3)–N(1)	1.960(5)	O(9)Li(3)N(5)	92.6(2)
Li(3)–N(5)	1.972(4)	O(1)Li(3)N(1)	92.52(2)	Li(3)–N(5)	1.985(4)	O(1)Li(3)N(1)	93.1(2)
XII				**XIII**			
La(1)–O(1)	2.330(1)	O(1)La(1)N(1)	67.43(4)	Sm(1)–O(1)	2.238(3)	O(1)Sm(1)N(1)	69.8(1)
La(1)–O(3)	2.404(1)	O(3)La(1)N(2)	64.69(4)	Sm(1)–O(3)	2.312(3)	O(3)Sm(1)N(2)	66.6(1)
La(1)–N(1)	2.721(1)	O(3)La(1)Na(1)	44.70(3)	Sm(1)–N(1)	2.630(4)	O(3)Sm(1)Na(1)	46.05(8)
La(1)–N(2)	2.823(1)	O(1)La(1)O(3)	140.04(4)	Sm(1)–N(2)	2.719(4)	O(1)Sm(1)O(3)	142.3(1)
Na(1)–O(3)	2.544(1)	N(1)La(1)N(2)	72.93(4)	Na(1)–O(3)	2.548(4)	N(1)Sm(1)N(2)	73.5(1)
La(1)···Na(1)	3.6092(9)			Sm(1)···Na(1)	3.533(3)		
XIV				**XIV**			
Sm(1)–O(3)	2.224(3)	Sm(2)O(7)Sm(1)	97.63(10)	Sm(2)–N(7)	2.561(4)		
Sm(1)–O(1)	2.347(3)	Sm(2)O(9)Sm(1)	97.41(9)	Sm(2)–N(5)	2.630(3)		
Sm(1)–O(5)	2.408(3)	Sm(1)O(5)Sm(2)	95.85(9)	Sm(2)–N(6)	2.678(3)		
Sm(1)–O(7)	2.429(3)	O(1)Sm(1)N(1)	71.51(10)	Li(1)–O(5)	1.966(8)		
Sm(1)–O(9)	2.443(3)	O(3)Sm(1)N(2)	68.56(10)	Li(1)–O(11)	2.007(8)		
Sm(2)–O(13)	2.216(3)	O(7)Sm(1)N(4)	70.90(10)	Li(1)–O(1)	2.095(8)		
Sm(2)–O(11)	2.325(3)	O(9)Sm(2)N(5)	69.53(10)	Li(1)–N(3)	2.113(8)		
Sm(2)–O(9)	2.406(3)	O(11)Sm(2)N(6)	67.71(10)	Sm(1)···Sm(2)	3.6429(3)		
Sm(2)–O(7)	2.411(3)	O(13)Sm(2)N(7)	71.29(11)				
Sm(2)–O(5)	2.499(3)	Li(1)O(5)Sm(1)	92.4(2)				
Sm(1)–N(1)	2.544(3)	Li(1)O(5)Sm(2)	91.1(2)				
Sm(1)–N(4)	2.599(3)	O(11)Li(1)O(1)	140.0(4)				
Sm(1)–N(2)	2.742(3)	O(5)Li(1)N(3)	90.8(3)				

coordination bond provides approaching the O atom in lithium phenoxide to the Ln atom and their further coordination interaction to form the binuclear fragment Li(μ-O)Ln. In turn, this bond provides approaching the Li atom to the second phenoxide ligand at the Ln atom, the formation of the second bridging O atom, and the formation of the final Li(μ-O)$_2$Ln group.

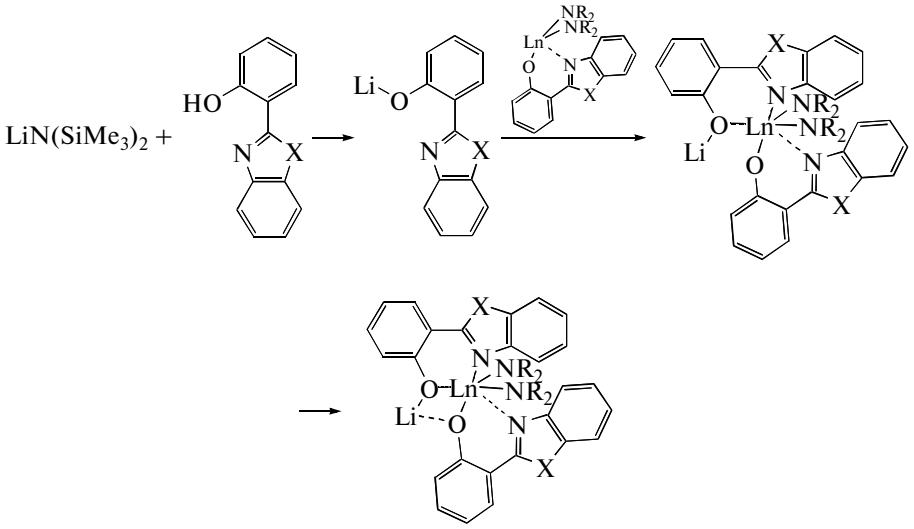

Scheme.

The proposed scheme is indirectly confirmed by the fact that the prolong heating of a mixture of Li(NpOON) with Tb_2(NpOON)$_6$ in THF does not afford complex **VII**.

The X-ray diffraction analysis of complexes **X, XI**, and **XII–XIV** show that, in all cases, the alkaline metal cation is bound to the lanthanide atom by the bridging oxygen atoms of the phenol or naphthol groups. This structure indicates that the synthesized compounds are closer in nature to the neutral heterobimetallic derivatives than to the ionic complexes with independent cationic and anionic fragments. Interestingly, the bilanthanoid structure obtained in all lanthanide complexes with the OON, SON, NpOON, and NpSON ligands [15–17] is retained in compound **XIV** only of the products considered.

The crystals of complexes **X** and **XI** are isostructural. The Y and Yb atoms in them have a distorted octahedral environment of six phenoxyl oxygen atoms (Fig. 1). The M–O distances are 2.240(2)–2.260(1) Å in compound **X** and 2.212(2)–2.234(2) Å in compound **XI**. The distinctions in the M–O distances between complexes **X** and **XI** are satisfactorily consistent with the difference in ionic radii of the metals (Y^{3+} (coordination number 6) 0.9 Å, Yb^{3+} (coordination number 6) 0.868 Å [27]). The Li cations are coordinated by two nitrogen and oxygen atoms of the adjacent OON ligands, due to which they have a distorted tetrahedral environment. The Li–O and Li–N distances are 1.931(4)–1.963(4) and 1.972(4)–2.034(4) Å in structure **X**, 1.882(4)–1.955(5) and 1.960(5)–2.019(4) Å in complex **XI**, respectively. The OON ligands in compounds **X** and **XI** are nearly planar. The dihedral angles between the phenoxyl and benzoxazole fragments are 0.77°–7.11° in compound **X** and 0.26°–7.03° in compound **XI**. Three pairs of the OON ligands in compounds **X** and **XI** are almost parallel to each other. The dihedral angles between the planes of these ligands range from 4.27° to 9.30° in compound **X** and from 4.68° to 9.79° in compound **XI**. The distances between the centers of the benzene rings (**A** and **B**, Fig. 1) of the OON ligands are 3.256–3.488 Å (**X**) and 3.250–3.476 Å (**XI**), indicating the π–π interactions between them [9]. Molecules of complexes **X** and **XI** in the crystalline state are isolated.

Complex **XIV** is a trinuclear cluster containing two Sm atoms and one Li atom. Each samarium atom is coordinated by one terminal and four bridging NpOON ligands (Fig. 2a), and the coordination number of samarium is 8. The Sm–O and Sm–N bond lengths are 2.216(3)–2.499(3) and 2.544(3)–2.678(3) Å, respectively. As expected, the terminal Sm(1,2)–O(3,13) bonds (2.224(3) and 2.216(3) Å) are noticeably shorter than analogous bridging bonds (2.325(3)–2.499(3) Å). The Sm–N distances are 2.544(3)–2.742(3) Å, and the range of their changing (~0.2 Å) appreciably exceeds a similar characteristic for complexes **X** and **XI**. The Li^+ cation is coordinated by three bridging ligands, one of which coordinates lithium through the bidentate mode (N,O; Li(1)–O(5) 1.966(8), Li(1)–N(3) 2.113(8) Å) and two others are coordinated through the monodentate mode (O-coordination, Li(1)–O(1) 2.095(8), Li(1)–O(11)

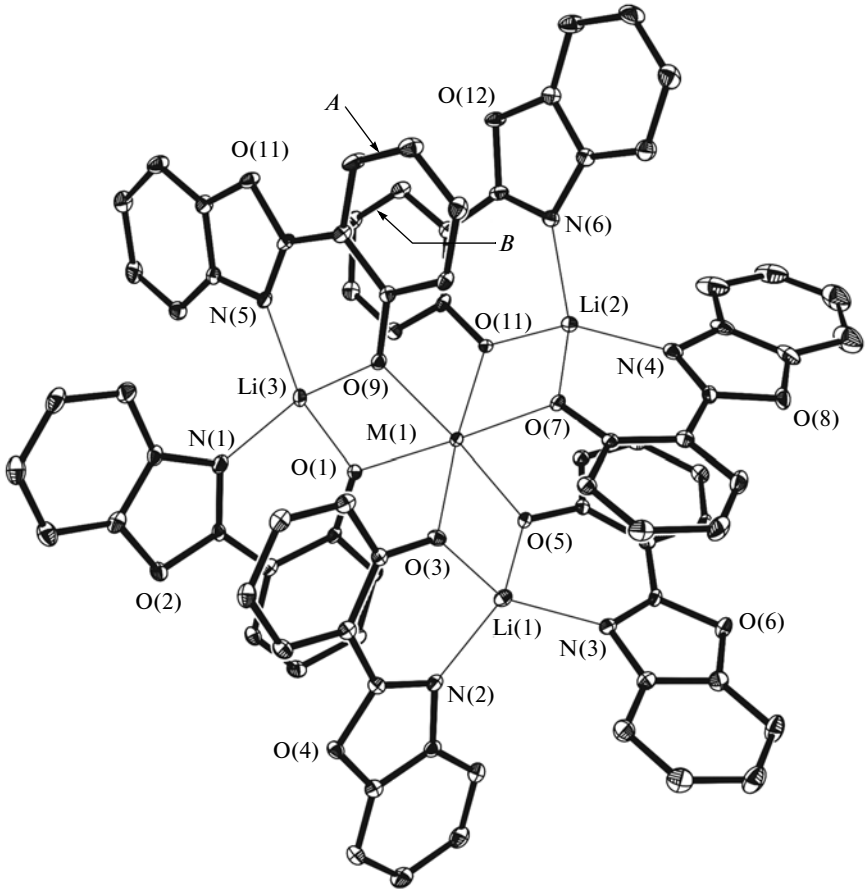

Fig. 1. Molecular structures of complexes **X** and **XI**. Thermal ellipsoids are given with 30% probability. M = Y (**X**) and Yb (**XI**).

2.007(8) Å). As a result, lithium has a trigonal pyramidal coordination.

Unlike the practically planar OON ligands in complexes **X** and **XI**, only one of the NpOON ligands (O(13,14)N(7)C(103–119)) in complex **XIV** is planar (the dihedral angle between the oxynaphthyl and benzoxazyl fragments is 4.32°), whereas others are noticeably nonplanar (the dihedral angles between the oxonaphthyl and benzoxazyl fragments are 9.54°–32.15°). In the crystal structure, molecules **XIV** form dimeric pairs due to intermolecular π–π interactions [28] (Fig. 3) involving the O(13,14)N(7)C(103–119) ligands of the adjacent molecules. The distance between the planes of the O(13,14)N(7)C(103–119) ligands is 3.281 Å and that between the centers of the benzene rings of these ligands is 4.122 Å (Fig. 2b). Perhaps, the π–π interactions result in the flattening of the O(13,14)N(7)C(103–119) ligand compared to other ligands.

The X-ray diffraction analysis of complexes **XII** and **XIII** show that their crystals are isostructural. The La and Sm atoms in these complexes are coordinated through the bidentate mode by two terminal and two bridging OON ligands (Fig. 3). The terminal bonds (La(1)–O(1) 2.330(1), La(1)–N(1) 2.721(1), Sm(1)–O(1) 2.238(3), and Sm(1)–N(1) 2.630(4) Å) are noticeably shorter than similar bonds in the bridging ligands (La(1)–O(3) 2.404(1), La(1)–N(2) 2.823(1), Sm(1)–O(3) 2.312(3), and Sm(1)–N(2) 2.719(4) Å). Unlike complexes **X**, **XI**, and **XIV**, in complexes **XII** and **XIII**, the Na^+ cations are coordinated by the oxygen atoms of the solvate DME molecules and two OON ligands. The OON ligands in complexes **XII** and **XIII** are nonplanar. The dihedral angles between the phenoxyl and benzoxazyl fragments are 16.41°, 19.55° in complex **XII** and 17.93°, 18.01° in complex **XIII**. In crystals these complexes are isolated.

The absorption spectra of phenoxides and naphthoxides **I–XIV** are similar and differ slightly from the spectra of analogous complexes containing no additional Li(XON) or Li(NpXON) fragments [15–17]. Figure 4 presents the absorption spectra of complexes **I** and **II** in a THF solution at ambient temperature. Both spectra contain the characteristic absorption bands of the aromatic groups at 210–400 nm. On going to the compounds of Y and lanthanides, the set of bands in the spectra remains unchanged but their intensities are insignificantly redistributed: the long-wavelength peaks somewhat increase in the spectra of the Sm, Tb, and Yb complexes.

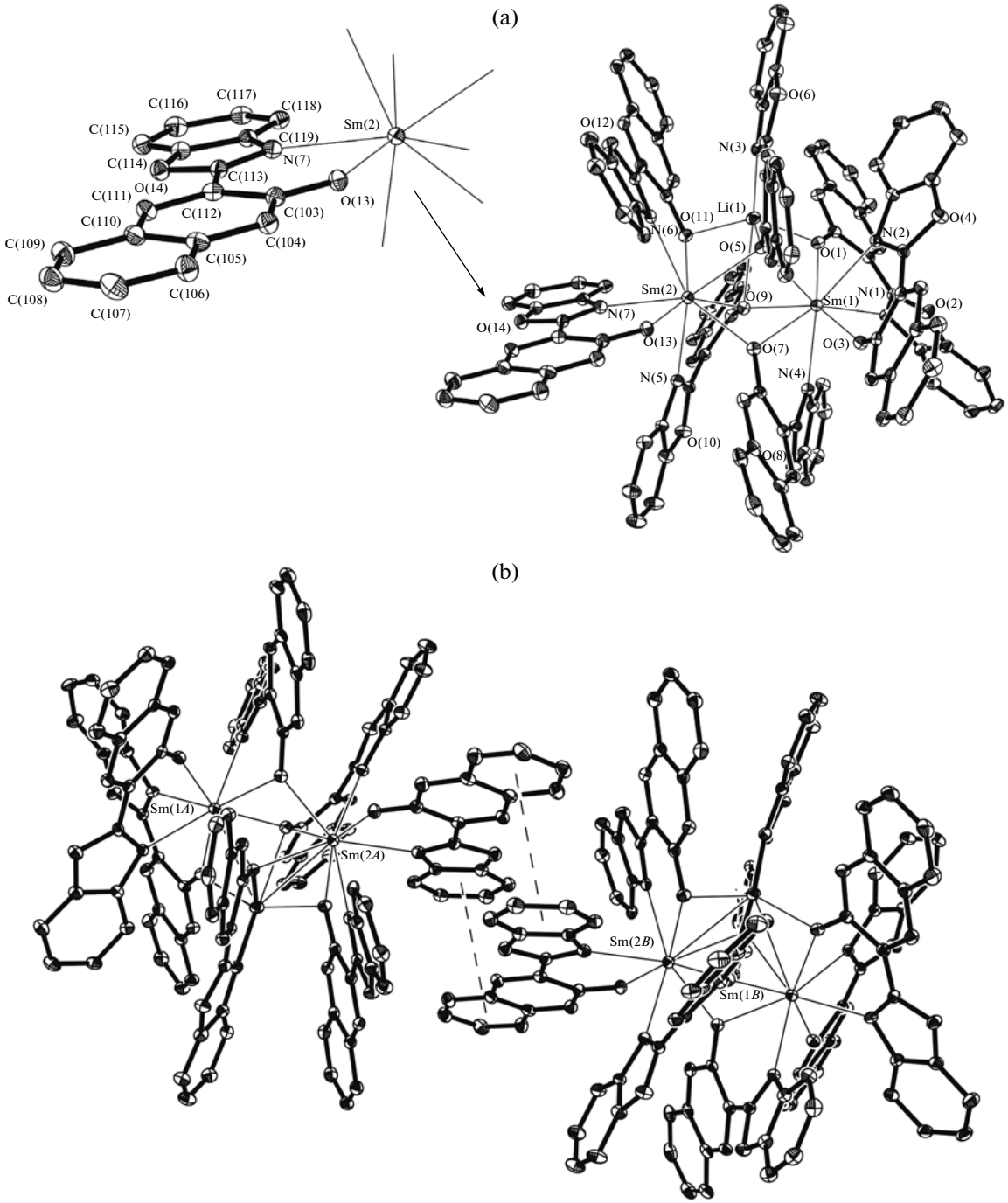

Fig. 2. (a) Molecular structure of complex **XIV** and (b) the packing fragment of complex **XIV**. Thermal ellipsoids are given with 30% probability.

All synthesized compounds in a THF solution exhibit the PL of the ligands as a broadened band at 430–460 nm (phenoxides, upon the excitation with the light at $\lambda_{ex} = 370$ nm) or 510–530 nm (naphthoxides, upon the excitation with the light at $\lambda_{ex} = 340$ nm). In addition, the spectra of samarium derivatives **XIII** and **XIV** in the visible range manifest weak bands of the *f–f* transitions, which are more distinctly seen in the spectrum of the terbium complex (**V**): 490, 550, 580, and 630 nm ($^5D_4 \rightarrow {}^7F_6$, $^7F_5$, $^7F_4$, $^7F_3$) (Fig. 5). The intensity of the luminescence bands of the ligands in the ate complexes considerably exceeds the intensity of the same bands in the analogs free of alkaline metals. The quantum yield is 52–100%.

In order to determine the EL properties of the synthesized complexes and to compare them with the

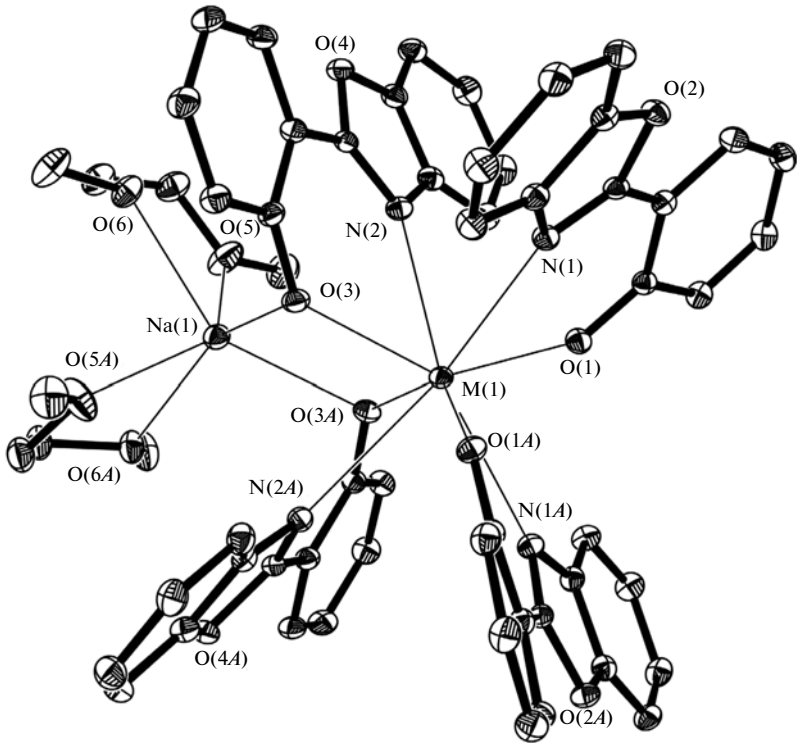

Fig. 3. Molecular structures of complexes **XII** (M = La) and **XIII** (M = Sm). Thermal ellipsoids are given with 30% probability.

properties of the earlier obtained neutral analogs [15–17], were prepared three-layer OLED devices of the same type in which these compounds were used as emission layers. The studies showed that the main working characteristics (the spectra, switch voltage, and volt–luminous and volt–ampere curves, Table 4) of the light-emitting diodes based on the ate complexes and their neutral analogs were similar. The highest difference is observed in light intensity. The emission intensity of the ligands in the ate complexes is by 20–30% higher than that in the neutral analogs, whereas the intensity of the metal-centered emission bands is noticeably lower. An especially strong decrease in the luminescence intensity of the metal (by 200 times) is observed for ytterbium complexes **VIII**, **IX**, and **XI**, which is likely due to a special excitation mechanism that occurs in the $Yb_2(XON)_6$ and $Yb_2(NpXON)_6$ complexes [26]. Complexes **X** and **XII** were not included into the table because of the low luminescence intensity. The character of the volt–luminous and volt–ampere curves (Fig. 6) and the zero response time indicate the absence of the expected dissociation of the complexes and ion diffusion in the electric field.

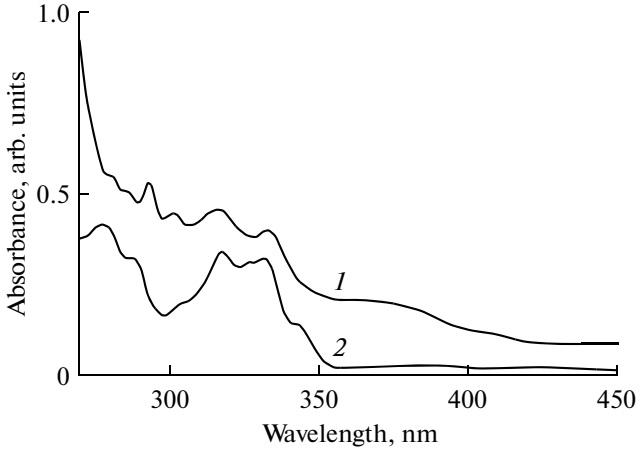

Fig. 4. Absorption spectra of complexes (*1*) **I** and (*2*) **II** in a THF solution (10^{-5} mol/L).

This behavior of the products is well consistent with their molecular structures, namely, the strong binding of the Li^+ cations with the Ln^{3+} ions by the double oxygen bridges preventing the dissociation of the molecules.

Thus, the photo- and electroluminescence properties of the lanthanide ate complexes with the (2-benzoxazol-2-yl)phenolate (or -naphtholate) and (2-benzthiazol-2-yl)phenolate (or -naphtholate) chelating ligands were studied. The study showed that the complexes contained no separated ions of the $[Ln(L)_4]^-[M]^+$ type and their behavior in the electric field almost did not differ from similar compounds containing no alkaline metal cations.

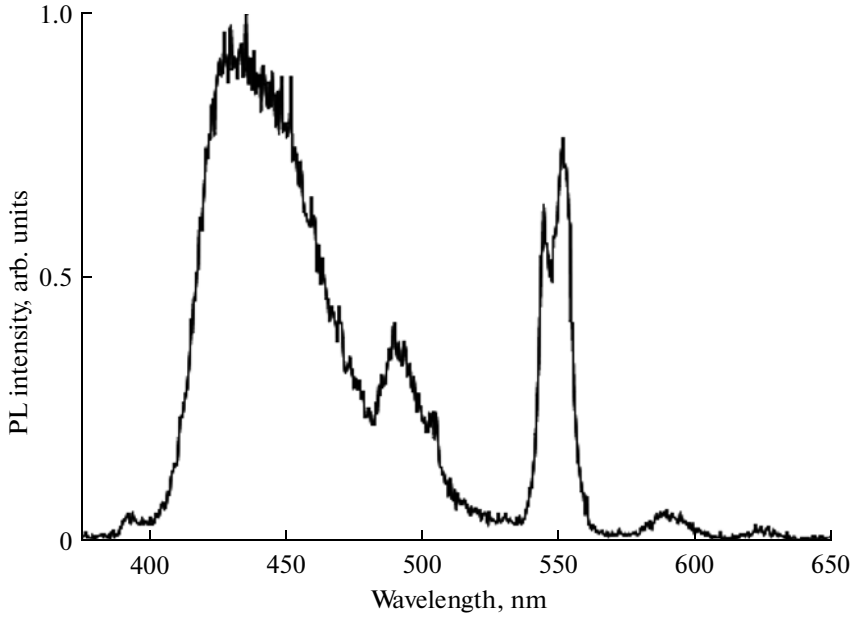

Fig. 5. PL spectrum of complex **V** in a THF solution (λ_{exc} = 345 nm).

Table 4. Working characteristics of the light-emitting diodes ITO/TPD/complex/Bath/Yb

Complex	Switch voltage, V	λ, nm	Maximum emission intensity[c], cd/m^2	Maximum efficiency		Quantum yield, %
				by current, cd/A	by power, Lm/W	
$Sc(OON)_4Li$ (I)	7[a]	499	35 (21)	0.11	0.08	0.06
$Sc(NpOON)_4Li$ (II)	4.5[a]	537	1100 (20)	1.52	0.9	0.8
$Y(NpOON)_4Li$ (III)	3.5[a]	533	1500 (20)	2.17	1.31	1.2
$Y(NpSON)_4Li$ (IV)	4.5[a]	572	490 (22)	0.5	0.32	0.3
$Tb(OON)_4Li(DME)$ (V)	8[a]	492, 548, 585, 620, 648	10 (27)	0.04	0.01	0.01
$Tb(SON)_4Li(DME)_2$ (VI)	7[a]	568	16 (20)	0.02	6×10^{-3}	$<1 \times 10^{-3}$
$Tb(NpOON)_4Li$ (VII)	7[a]	526	11 (22)	0.01	4×10^{-3}	$<1 \times 10^{-3}$
$Yb(NpOON)_4Li$ (VIII)	5[b]	526, 979	70 (28), 85[d]	0.03	0.07[e]	0.25
$Yb(NpSON)_4Li$ (IX)	7[b]	570, 979	6 (21), 220[d]	0.01	0.36[e]	0.4
$Yb(OON)_6Li_3$ (XI)	9[b]	502, 979	14 (26), 93[d]	0.03	0.2[e]	0.32
$Sm(OON)_4Na(DME)_2$ (XIII)	5.5[a]	503, 566, 604, 649, 710	200 (21.5)	1.05	0.5	0.4
$Sm_2(NpOON)_7Li$ (XIV)	7[a]	530	25 (26.5)	0.02	8 ¥ 10^{-3}	0.01

[a] Voltage at 1 cd/m^2.
[b] Voltage at 1 mA/cm^2.
[c] The value in parentheses is the voltage (V) at which the maximum emission intensity was obtained.
[d] Dimensionality is μW/cm^2.
[e] Dimensionality is mW/W.

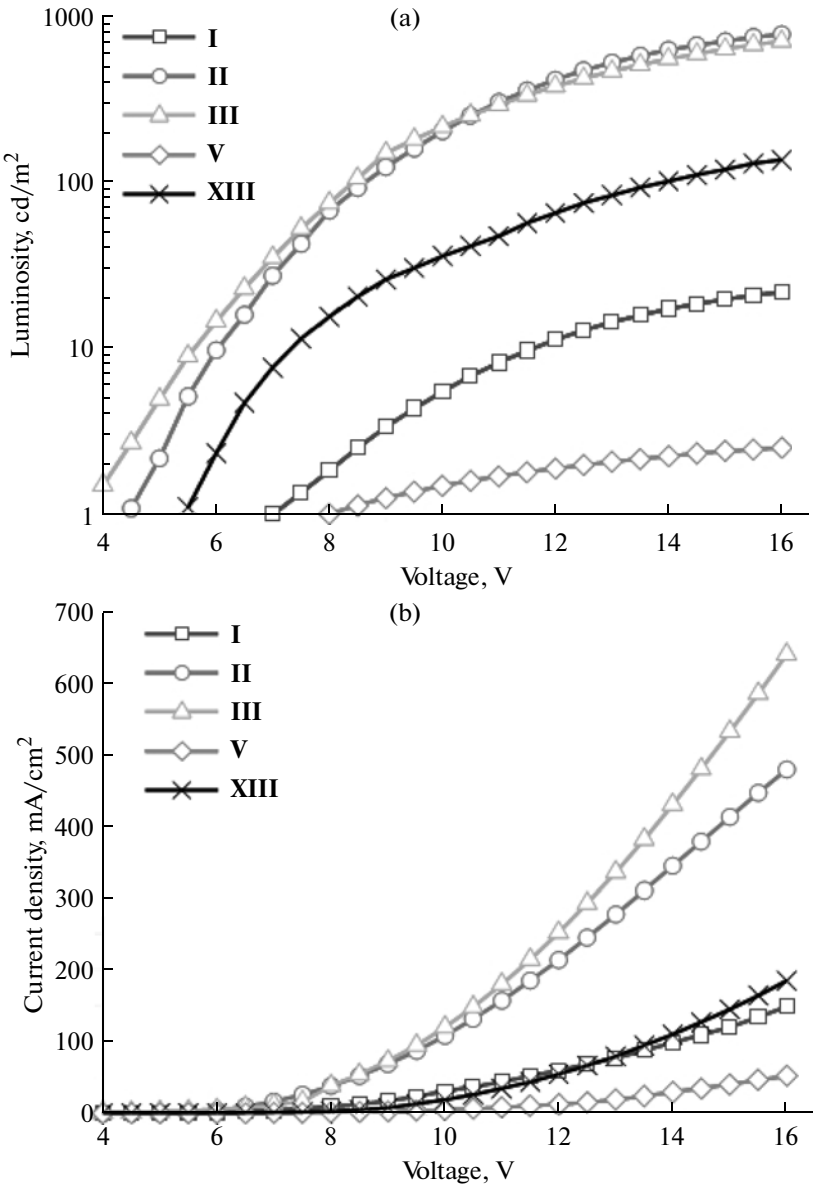

Fig. 6. (a) Volt–luminous and (b) volt–ampere curves of the OLED devices based on compounds **I**, **II**, **III**, **V**, and **XIII**.

ACKNOWLEDGMENTS

The authors are grateful to M.A. Lopatin for the recording and discussion of the electronic spectra.

This work was supported by the Presidium of the Russian Academy of Sciences (program "Foundations for Basic Research of Nanotechnologies and Nanomaterials"), the Russian Foundation for Basic Research (project nos. 13-03-00097, 13-03-00891, and 12-03-31273mol_a), and the Ministry of Education and Science of the Russian Federation (agreement 8637).

REFERENCES

1. New, E.J., Parker, D., Smith, D.G., and Walton, J.W., *Curr. Opin. Chem. Biol.,* 2010, vol. 14, p. 238.
2. Egorova, A.V., Skripinets, Yu.V., Aleksandrova, D.I., and Antonovich, V.P., *Metody i ob"ekty khim. analiza*, 2010, vol. 5, p. 180.
3. Hovinen, J. and Guy, P.M., *Biocojugate Chem.,* 2009, vol. 20, p. 404.
4. Hagan, A.K. and Zuchner, T., *Anal. Bioanal. Chem.*, 2011, vol. 400, p. 2847.
5. Binnemans, K., *Chem. Rev.*, 2009, vol. 109, p. 4283.
6. Eliseeva, S.V. and Bunzli, J.-C., *Chem. Soc. Rev.*, 2010, vol. 39, p. 189.

7. Bochkarev, M.N., Vitukhnovskii, A.G., and Katkova, M.A., in *Organicheskie svetoizluchayushchie diody (OLED)* (Organic Light-Emitting Diodes (OLED)), Nizhnii Novgorod: DEKOM, 2011.
8. Pei, Q.B., Yu, G., Zhang, C., and Heeger, A.J., *Science*, 1995, vol. 269, p. 1086.
9. deMello, J.C., Tessler, N., Graham, S.C., and Friend, R.H., *Phys. Rev., B*, 1998, vol. 57, p. 12951.
10. Bernhard, S., Barron, J.A., and Houston, P.L., *J. Am. Chem. Soc.*, 2002, vol. 124, p. 13624.
11. Yang, C.-H., Beltran, J., Lemaur, V., and Cornil, J., *Inorg. Chem.*, 2010, vol. 49, p. 9891.
12. Armaroli, N., Accorci, G., and Michel, H., *Adv. Mater.*, 2006, vol. 18, p. 1313.
13. Bernhard, S., Gao, X., Malliaras, G.G., and Abruña, H.D., *Adv. Mater.*, 2002, vol. 14, p. 433.
14. Bochkarev, M.N., Zakharov, L.N., and Kalinina, G.S., *Organoderivatives of Rare Earth Elements*, Dordrecht: Kluwer Academic, 1995.
15. Balashova, T.V., Pushkarev, A.P., and Ilichev, V.A., *Polyhedron*, 2013, vol. 50, p. 112.
16. Katkova, M.A., Pushkarev, A.P., and Balashova, T.V., *J. Mater. Chem.*, 2011, vol. 21, p. 16611.
17. Burin, M.E., Kuzyaev, D.M., Lopatin, M.A., et al., *Synth. Met.*, 2013, vol. 164, p. 55.
18. Bochkarev, M.N., Fagin, A.A., Druzhkov, N.O., et al., *J. Organomet. Chem.*, 2010, vol. 695, p. 2774.
19. Burin, M.E., Kuzyaev, D.M., Lopatin, M.A., et al., *Synth. Met.*, 2013, vol. 164, p. 55.
20. Katkova, M.A., Pushkarev, A.P., Balashova, T.V., et al., *J. Mater. Chem.*, 2011, vol. 21, p. 16611.
21. *SAINT Plus. Data Reduction and Correction Program. Version 6.02a*, Madison (WI, USA): Bruker AXS, 2000.
22. *Data Collection. Reduction and Correction Program. CrysalisPro Software Package*, Agilent Technologies, 2012.
23. Sheldrick, G.M., *SADABS. Version 2.01. Bruker/Siemens Area Detector Absorption Correction Program*, Madison (WI, USA): Bruker AXS, 1998.
24. *SCALE3 ABSPACK: Empirical Absorption Correction. CrysalisPro Software Package*, Agilent Technologies, 2012.
25. Sheldrick G.M., *SHELXTL. Version 6.12. Structure Determination Software Suite*, Madison (WI, USA): Bruker AXS, 2000.
26. Pushkarev, A.P., Il'ichev, V.A., and Balashova, T.V., *Izv. Akad. Nauk, Ser. Khim.*, 2013, no. 2, p. 395.
27. Shannon, R.D., *Acta. Crystallogr., Sect. A: Cryst. Phys., Diffr., Theor. Gen. Crystallogr.*, 1976, vol. 32, p. 751.
28. Janiak, C., *Dalton Trans.*, 2000, p. 3885.

Translated by E. Yablonskaya